



UNITED NATIONS  
UNIVERSITY

**UNU-GTP**

Geothermal Training Programme

Orkustofnun, Grensasvegur 9  
IS-108 Reykjavik, Iceland

Reports 2019  
Number 26

## **TEMPERATURE CONDITIONS AND RESOURCE ASSESSMENT OF LOW- TO MEDIUM-TEMPERATURE CONVECTIVE GEOTHERMAL SYSTEMS IN JIAODONG PENINSULA, CHINA**

**Shi Meng**

UNU Geothermal Training Programme  
Shandong No. 3 Exploration Institute of Geology and Mineral Resources  
271 Airport Road, Zhifu District 264000  
Yantai  
CHINA  
*495746716@qq.com*

### **ABSTRACT**

The structural units in the Jiaodong peninsula mainly consist of the Jiaobei uplift, the Jiaolai basin and the Weihai uplift. The heat flow in the Jiaodong peninsula, based on silica temperature, shows that the Jiaobei uplift and the Weihai uplift areas have higher heat flow than the Jiaolai depression basin, and that the closer you get to the centre of the axis of the uplift area, the higher the heat flow becomes. The lithology of the uplift area is mainly composed of intrusive and metamorphic rocks with high thermal conductivity and permeability, while the lithology of the depression basin is dominated by sandstone with low thermal conductivity and low permeability. Therefore, the bottom of the Jiaolai basin acts like an insulating cap or roof, both for heat and water flow, which causes the heat flow pattern to be different in different structural units. In order to visualize the heat flow distribution more clearly, a 3D temperature model of the Weihai uplift area has been constructed using Leapfrog. In addition to the Wenquan fault having a higher temperature, the fault is the main structure controlling the hot spring and heat flow distribution in this area. A lumped parameter model was used to simulate the water level response to variable production in the Yujia Tang geothermal field. The results show that if the production is increased to about 15 times the current production, the water level will drop by 180 m, which should still be manageable. The volumetric method was used to estimate the geothermal production potential of the Wenquan Tang and Dong Tang geothermal fields, showing that the thermal energy production potential of these two areas is more than 2-3 MWth each (P90 estimate).

### **1. INTRODUCTION**

Low- to medium-temperature convective geothermal systems are widely distributed in China, especially in the eastern coastal area affected by collision of crustal plates. They have no specific heat sources, such as intrusions, other than the regular crustal heat content, but are mainly located in fracture zones with normal or slightly higher background heat flow. As early as the 1980s, Chinese scholars began to systematically study the geothermal heat flow. Later, scientists started using numerical simulation methods to simulate the geothermal temperature field and proposed the deflection and redistribution of

terrestrial heat flow as an explanation for anomalies such as geothermal systems (Zhang et al., 1982; Xiong and Zhang, 1984). Xie and Yu (1988) summarized the temperature field characteristics of the Sichuan basin using temperature data from 460 wells in the basin, proposing that the temperature of the uplift region at the interface between the marine stratum and the continental stratum is higher than normal, and that the temperature is lower in the depressions. This is mainly due to the fact that the uplift and depression in the same tectonic zone have different structural forms. This difference causes a redistribution of the heat flow in the layer. Chen et al. (1990) explored the relationship between geothermal and geological structures and the tectonic-thermal evolution history using the temperature and terrestrial heat flow results for the North China basin. Hu and Wang (1994) conducted a comprehensive study of the terrestrial heat flow characteristics of numerous orogenic belts using 125 reliable datasets from south-eastern China. It was found that the heat flow distribution was significantly affected by the thermal conductivity structure of the shallow crust.

On the basis of previous studies on the characteristics of terrestrial heat flow in recent years, many geologists have focused their research on heat flow characteristics and lithospheric thermal structure in various regions of China, such as the Qaidam basin, the Tarim basin, the northern margin of the South China Sea, the Sichuan basin, the Bohai Bay basin and others (Li et al., 2016; Liu et al., 2017; Shi et al., 2017; Xie and Yu, 1988; Qiu et al., 2017). These authors discuss the effects of thermal properties of rocks and fracture development on the current temperature field. Based on the previous research results, this report takes the geothermal systems of Jiaodong peninsula as an example to analyse the regional geology and structure, wellbore temperature data, the temperature field, different thermal properties of rocks, fluid chemistry and long-term monitoring data. The characteristics and relationship of the temperature field between the Jiaobei uplift, the Jiaolai depression and the Weihai uplift are discussed systematically and a heat flow model is proposed as well as a conceptual model suitable for the Jiaodong peninsula. A lumped parameter model was used to simulate the water level response to variable production rates and the volumetric method was used to calculate the thermal energy in the reservoir. The characteristics of the temperature field distribution, heat flow variations, heat source of geothermal fluids as well as the water level response to production and thermal energy in Jiaodong Peninsula are also studied.

## 2. BACKGROUND

### 2.1 Geological and tectonic setting

Jiaodong is located on the eastern margin of the North China craton, belonging to the Pacific Ocean tectonic area, and is part of the Pacific rim tectonic-magmatic activity belt (Figure 1).

In addition to the wide distribution of geothermal resources, gold deposits are huge in Jiaodong peninsula. The most important common feature of geothermal resources and gold resources is that they are both controlled by regional faults. The widely distributed regional faults not only provide the tectonic

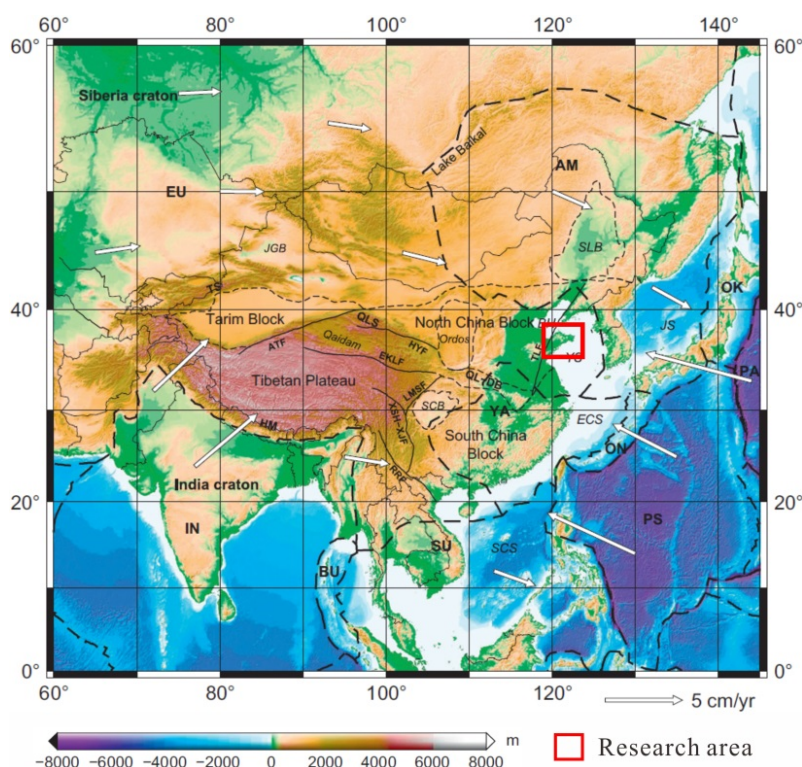


FIGURE 1: Location of Jiaodong peninsula, the research area (modified from Chen et al., 2013)

space and migration channels for gold deposits (Lv et al., 2015), but also provide channels for the deep migration and up-flow of geothermal liquids (Jin et al., 1999; Zhang, 2011). The previous studies of the mineralization mechanism of gold resources also included detailed research of the basic geology and structure of the Jiaodong peninsula and provided detailed geological data for the study of the heat flow model of the geothermal resources on Jiaodong peninsula.

This area has many medium-intensity intrusive rocks caused by oceanic subduction from the Jurassic to the early Cretaceous (Liu et al., 2018) and the dykes are highly developed. The intrusive rocks were formed in different periods with an average density of 10 intrusions per km<sup>2</sup> and there is no obvious mixing influence from crustal material during the ascent which originated from the lithospheric mantle rather than the asthenosphere mantle (Tan et al., 2006; Long, 2017).

During the Archean-Proterozoic, the crystalline basement in this area was formed. The Palaeozoic was the formation period of the sedimentary caprock of the platform. Before this period, the Jiaodong peninsula was a stable continental block and the terrestrial heat flow was low prior to the destruction of the North China craton and lithospheric thinning (Lin et al., 2013); The Mesozoic and Cainozoic eras are important stages of intense crustal activity in Jiaodong. Especially during the Yanshanian period, the upper mantle is strongly active accompanied by crustal movement, forming a series of NE-SW and NNE-SSW trending compressive-torsional faults and NW-SE trending tensional faults. The faults are considered secondary faults in the regional Tanlu fault zone (Mao et al., 2005). The regional Muping-Jimo fault zone, for example, controls the boundary of the Jiaolai basin, and its extension in the Cretaceous controlled the formation and development of the Jiaolai basin (Zhang and Zhang, 2007). The Taocun fault is a deep-cut fault cutting the Moho surface shown by seismic detection (Pan et al., 2015). The tectonic activities and intrusive rocks determine the distribution of tectonic units in the Jiaodong peninsula which divides the Jiaodong block into three structural units: the Jiaobei uplift, the Weihai uplift and the Jiaolai depression. The geology, structure, thermal properties of the rocks and the crustal structure between these three different structural units indirectly provide the background for geothermal activity on the Jiaodong peninsula.

It can be seen from Figure 2 that the lithology of the Jiaobei uplift and the Weihai uplift is mainly composed of Archean and Proterozoic metamorphic rocks and Mesozoic intrusive rocks. The lithology of the Jiaolai basin is mainly Cretaceous sandstone and the thickness of sediments in some areas is more than 7 km. The depth of the detachment system, which controls the origin of Jiaolai basin, is 8-10 km (Zhang et al., 2006). The sedimentary age of the Wawukuang formation at the bottom of Jiaolai basin is early Cretaceous, the sediments mainly comes



FIGURE 2: Regional geological map of Jiaodong peninsula



from the denudation-transport-deposition of metamorphic rocks in the early Jiaobei uplift and Weihai uplift.

## 2.2 Geothermal manifestations

The structural units in the study area mainly consist of the Jiaobei uplift, the Jiaolai basin and the Weihai uplift. The main structural traces include the Rushan-Weihai anticline, the Qixia anticline, and the Jiaolai syncline. An anticline is a "ridge-type" structure with a narrow upper section and a wide lower part which is beneficial to the lateral migration of geothermal fluid and transport. The overall strike of the faults is consistent with the strain effect on the edge of the Eurasian and Pacific plates and easily causes earthquakes (Deng et al., 1999; Chen et al., 2004; Zhang et al., 2007). The NE-SW and NNE-SSW trending faults are mainly compressive faults and torsional faults which mainly transport heat, the NW-SE faults are mainly tensional or tensional-shear faults and mainly transport water (Lv et al., 2007). The geothermal resources on the Jiaodong peninsula are mainly distributed in a "V" shaped area where the hanging walls of the NE-SW and NW-SE trending faults intersect each other. The geothermal reservoir is controlled by the NE-SW and NW-SE trending faults and has an irregular columnar shape. Figure 3 shows that the A-A' and B-B' are different trending faults, the fault A-A is water conducting and B-B' is thermal conducting. The surface water seeps into the crust entering the deep circulation. When the water reaches the intersection of the two faults, the water is heated by heat convection and conduction and flows up along the fracture zone.

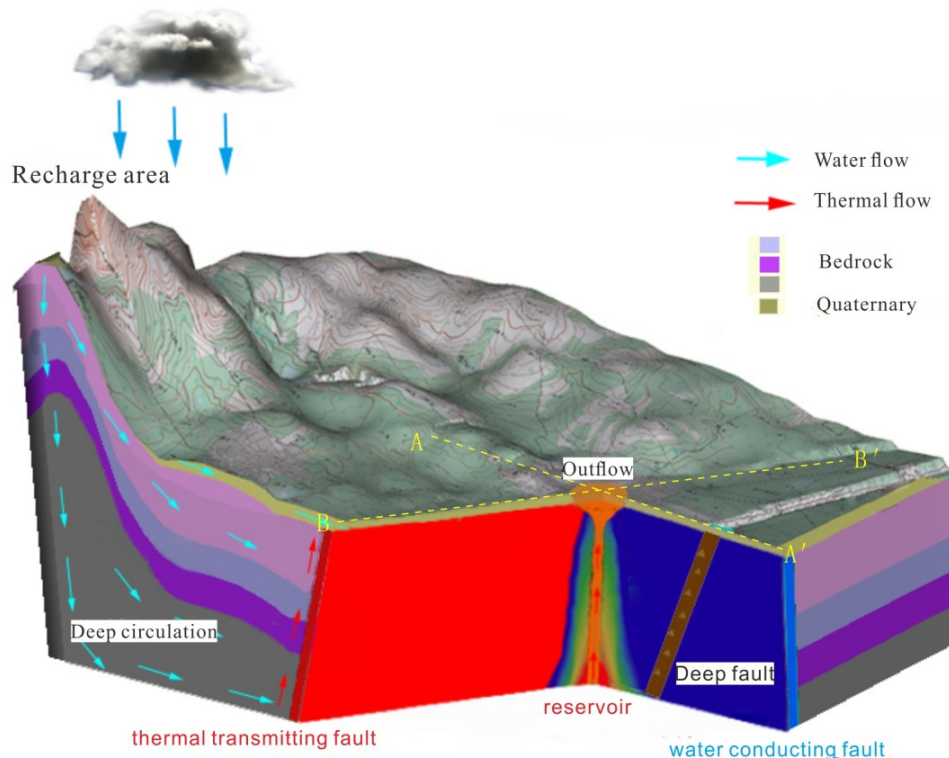


FIGURE 3: Simple conceptual sketch of a fracture controlled geothermal system

## 3. TEMPERATURE DATA

### 3.1 Reservoir temperature based on silica content

Terrestrial heat flow is considered to be an important parameter for studying the geodynamic process of the formation and evolution of orogenic belts. Different tectonic units have different background heat flow due to different tectonic-thermal evolution history (Hu and Wang, 1994). Terrestrial heat flow is

also important for understanding the regional temperature field. Jiaodong peninsula lies in the high heat flow zone on the west coast of the Pacific rim, which is the junction zone between the North China plate and the Yangtze plate. Structures and intrusive rocks are well developed which provides a favourable environment for the formation, conduction and storage of geothermal resources. In general, the Jiaodong peninsula was a stable rock platform before the Mesozoic, and the terrestrial heat flow value of the whole Jiaodong peninsula was low. Since the Mesozoic, Jiaodong entered the stage of rift development and a slow warming process began. From the Late Cretaceous to the Early Tertiary, temperature in the Jiaodong peninsula increased. Since the Late Tertiary, temperature in the Jiaodong peninsula has gradually begun to decline, but still retains the high geothermal background from the previous period (Chen et al., 1988).

The sub terrain temperature can reflect the characteristics of the thermal energy in the upper crust. The study of the temperature can, therefore, enhance the understanding of the distribution of thermal energy in that part of the crust. Li et al. (1997) mapped the heat flow at a resolution of 1:200 000 and made a contour map of the Jiaodong peninsula based on the SiO<sub>2</sub> values of 578 reliable water samples in the area (Figure 4). In Figure 5 it can be seen that the heat flow values in the Jiaobei uplift and Weihai uplift are obviously higher than in the Jiaolai depression. The heat flow in the uplift area, based on silica temperatures, is generally greater than 60 mW/m<sup>2</sup> with the highest value being 85 mW/m<sup>2</sup>, while the heat flow in the depression is generally lower than 60 mW/m<sup>2</sup>. Compared with the geothermal heat flow value of 47.2 mW/m<sup>2</sup> for North China, the Jiaodong peninsula has a higher background value of terrestrial heat flow, especially in the anticlinal axis of the Jiaobei uplift and Weihai uplift where the heat flow is above 80 mW/m<sup>2</sup>. The regional distribution of high heat flow values shows NE-SW and NNE-SSW alignments which are basically consistent with the strike of the NE-SW and NNE-SSW faults on the Jiaodong peninsula. Meanwhile, it can be seen that the average heat flow value decreases

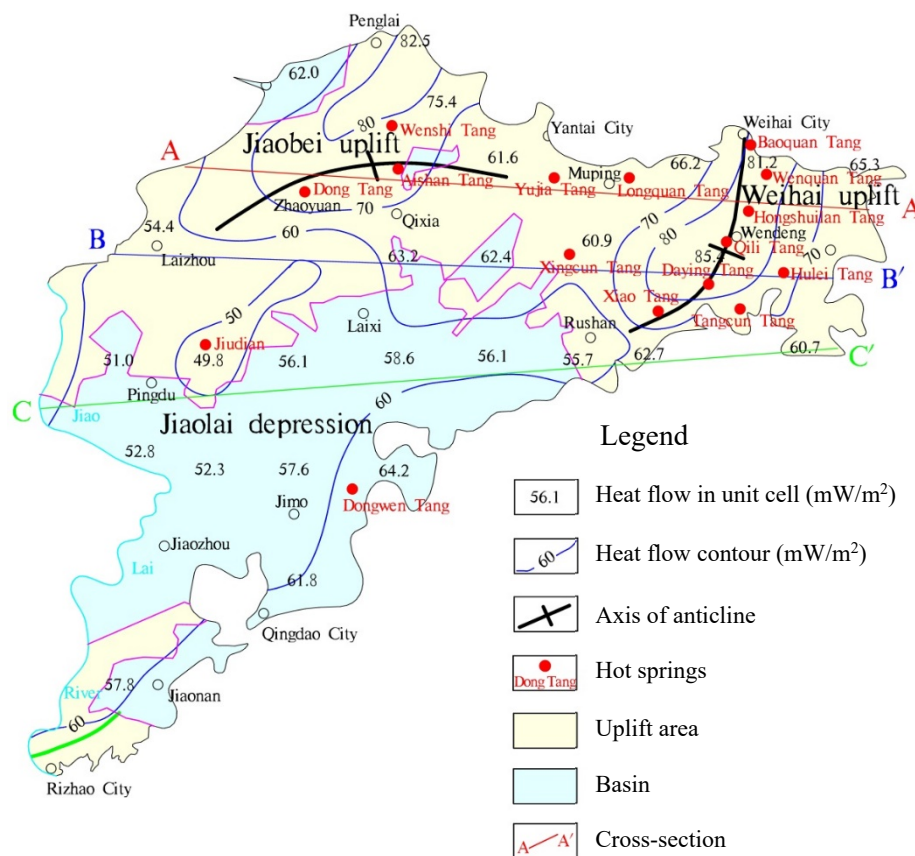


FIGURE 4: Heat flow distribution map for the Jiaodong peninsula based on silica temperatures (modified from Li et al., 1997)

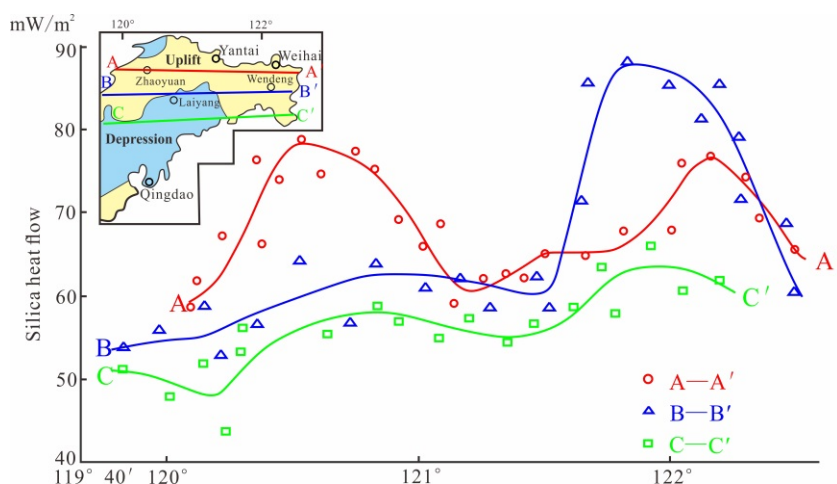


FIGURE 5: Cross-sections showing heat flow according to silica temperatures (see Figure 4) (modified from Li et al., 1997)

gradually with increasing distance of the sampling point from the anticlinal axis until the regional average heat flow is reached.

The temperatures of natural hot springs on the Jiaodong peninsula show that the closer the hot spring is to the centre of the axis of the uplift area, the higher the temperature. Baoquan Tang (67°C), Hongshuilan Tang (71°C) and Qili Tang (66°C) are hot springs located along the axis of the Weihai uplift area and

have obviously higher temperature than the Tangcun Tang (51°C) and Xingcun Tang hot springs (30°C) which are located farther from the axis. The temperature of Xingcun Tang hot spring, which is located near the contact zone between the Jiaolai basin and the Weihai uplift, is only 30°C (Table 1). This emphasises the differences in the surface heat flow between different tectonic units such as the Jiaobei uplift, the Jiaolai basin and the Weihai uplift. The terrestrial heat flow in different regions of the same tectonic unit varies also.

TABLE 1: Geothermal reservoir characteristics on the Jiaodong peninsula

Name of spring	SiO <sub>2</sub> (mg/L)	Silica temp. (°C)	Spring temp. (°C)	Name of spring	SiO <sub>2</sub> (mg/L)	Silica temp. (°C)	Spring temp. (°C)
Baoquan Tang	67.69	115	67	Longquan Tang	59.0	109	59
Wenquan Tang	85.54	126	59	Yujia Tang	69.5	116	46
Hongshuilan Tang	105.00	135	71	Xingcun Tang	63.8	113	28
Qili Tang	105.00	135	66	Dongwen Tang	82.4	124	62
Hulei Tang	108.54	137	60	Aishan Tang	70.8	117	52
Tangcun Tang	54.85	106	51	Wenshi Tang	98.7	132	54
Daying Tang	58.77	109	62	Dong Tang	89.6	128	81
Xiao Tang	60.62	110	56	Jiudian	103.6	136	61

### 3.2 Temperature logs

In order to search for more geothermal fields on the Jiaodong peninsula, many boreholes were drilled in the past decade without finding a geothermal resource. Temperature logs from 16 wells are available to estimate the temperature gradient in the area. The temperature logging was made days after the drilling activities ended, thus the temperature is considered to be semi stable. Figure 6 shows the position of the wells in the area and Figure 7 shows the temperature logs.

In order to better compare the difference between wells in geothermal fields and wells outside of geothermal fields, the Yujia Tang hot spring is used as a contrast (no. 13) in Figures 6 and 7. From Figure 7 it can be seen that the temperature does not increase linearly with depth in wells inside geothermal fields while the temperature logs in wells outside of geothermal fields are linear. This means that outside geothermal fields, there are no obvious anomalies in the geothermal gradient, it is mainly normal terrestrial heat flow heating the groundwater. The temperature gradient outside of geothermal fields mainly ranges from 19 to 23°C/km.

Figure 8 shows the lithology and temperature of the Zangnan well (no. 14 in Figures 6 and 7). It shows that the rock type of the cap is gravel sand and that the cap is very thin, only about 10 m. The lithology consists mainly of monzonitic granite. In fact, on the Jiaodong peninsula, the cap rocks of the geothermal fields are mainly gravel sand and they are very thin, most less than 50 m.

Boreholes outside geothermal fields have linear geothermal gradient. No high-temperature heat source such as magma was found in this area and no obvious geothermal heat anomalies were found in the deep crust since most of the heat anomalies in the boreholes come from geothermal fluids. The main heat source of the water is terrestrial heat flow and heat-conducting faults.

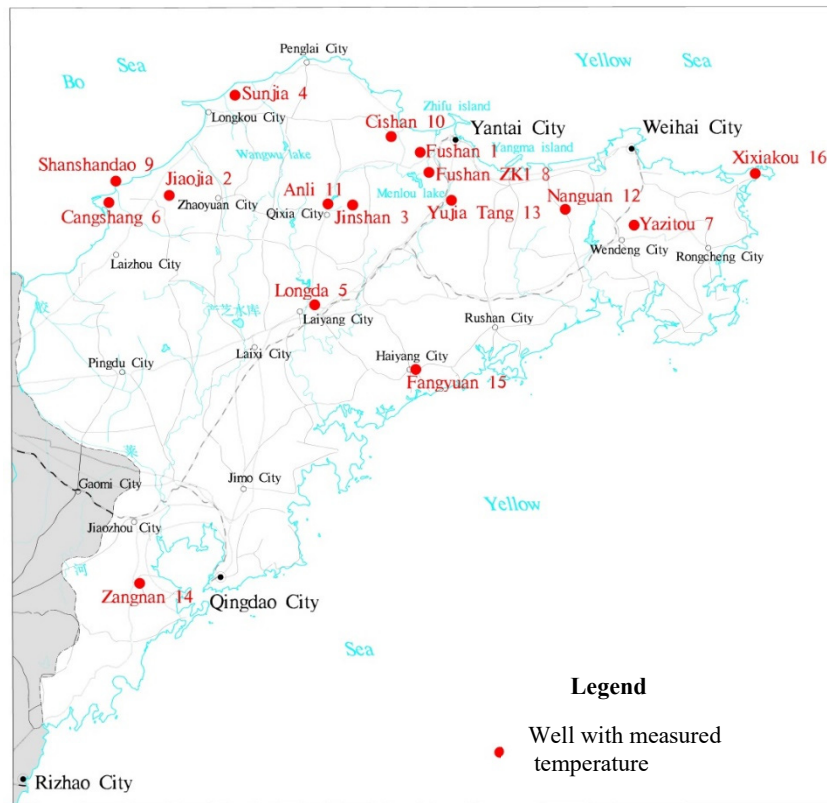


FIGURE 6: Location of wells which were logged for temperature (see Figure 7).

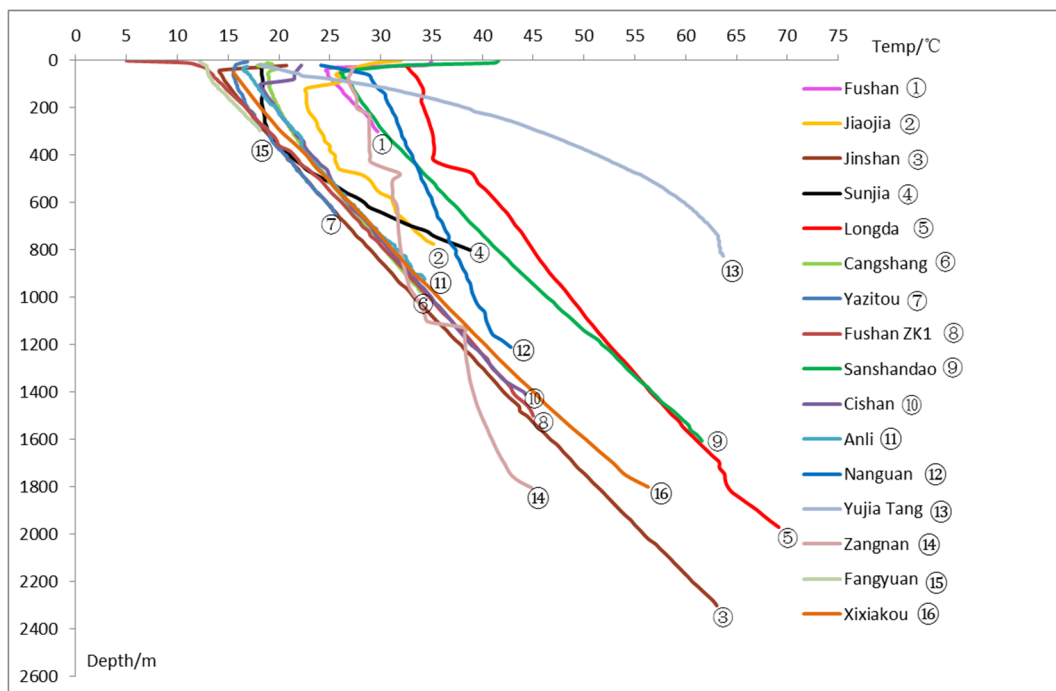


FIGURE 7: Temperature logs in wells (for location see Figure 6)



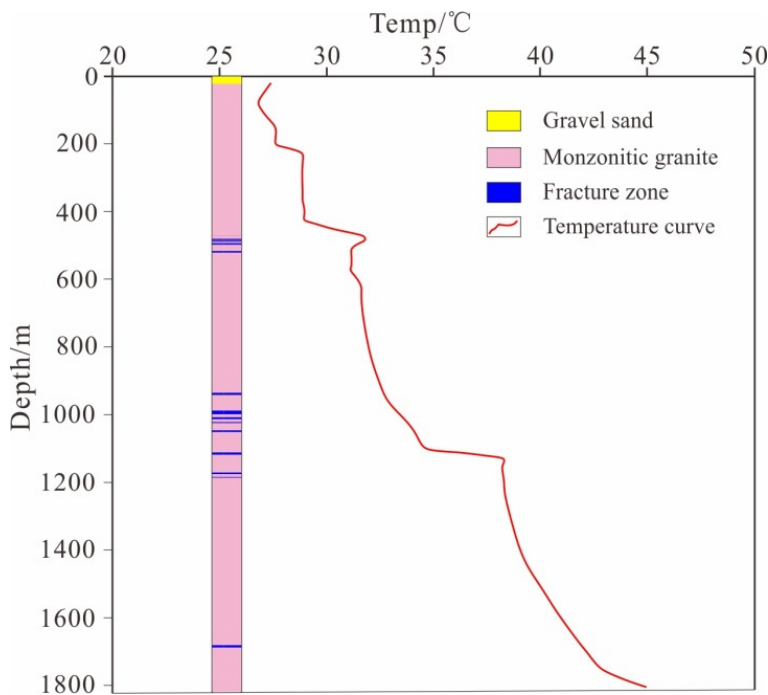


FIGURE 8: Temperature log and lithology in the Zangnan well (no. 14 in Figures 6 and 7)

### 3.3 Flow patterns

In order to study the reservoir temperature characteristics on the Jiaodong peninsula, samples were taken from 16 natural hot springs to preliminarily determine their chemical composition and estimate temperature. Due to the mixing with seawater, water samples from some hot springs did not only have a large amount of  $\text{Cl}^-$  but also of  $\text{Na}^+$  and  $\text{K}^+$ . The  $\text{Na}^+$ ,  $\text{K}^+$  and other cations are not easily balanced with the surrounding rock. Therefore, this study abandons the method of using cation temperatures and uses  $\text{SiO}_2$  temperature only (silica temperature) to estimate reservoir temperatures.

The formula for calculating reservoir temperature  $T$  ( $^{\circ}\text{C}$ ) based on  $\text{SiO}_2$  concentration is as follows (Fournier, 1977):

$$T(^{\circ}\text{C}) = \frac{1522}{5.75 - \text{Log } S} - 273.15 \quad (1)$$

where  $S$  is the concentration of  $\text{SiO}_2$  in water (mg/L)

According to the  $\text{SiO}_2$  temperature, the reservoir temperature ranges between 106 and 137 $^{\circ}\text{C}$  (Table 1), i.e., all reservoir temperatures are lower than 150 $^{\circ}\text{C}$  making this a low- to medium-temperature geothermal system. This means there is no high-temperature heat source in the area like a magmatic intrusion, through which geothermal water flows. The heat of the geothermal liquids mainly comes from:

- 1) Hydrothermal convection in thermal conductive faults;
- 2) Heat conduction by terrestrial heat flow; and/or
- 3) Conduction-convection during groundwater migration.

## 4. 3D GEOTHERMAL MODEL

*Leapfrog Geothermal* is a 3D modelling, visualisation and resource management software, developed by ARANZ Geo (Applied Research Associates Ltd) with geoscientific input from GNS Science, to meet the 3D computing needs of the geothermal industry. Leapfrog Geothermal is based on implicit modelling methods that represent geology, structure, geophysical and reservoir data with fitted mathematical functions. Complex geological models are built by combining measured field data, specialist interpretation and user editing. The leapfrog software is easy to use and allows 3D models to be built up quickly and efficiently as well as being routinely updated (Alcaraz et al., 2011).

Figure 9 shows the Weihai uplift area and the heat distribution of the hot springs and wells on the Jiaodong peninsula.



### 4.1 Data compilation

Before modelling the Weihai uplift area, the surface and lithological data were analysed. Surface data including a surface elevation map, a geological map, a structural map and well locations were the input for Leapfrog, including the boundaries of the research area. The lateral temperature distribution at shallow depth was based on borehole data. Subsurface data was derived from previous surveys. The information (including lithology, alteration, casing depth, directional survey data, and PTS logging data) (Wulaningsih et al., 2017) was used to construct the well trajectories in the 3D model.

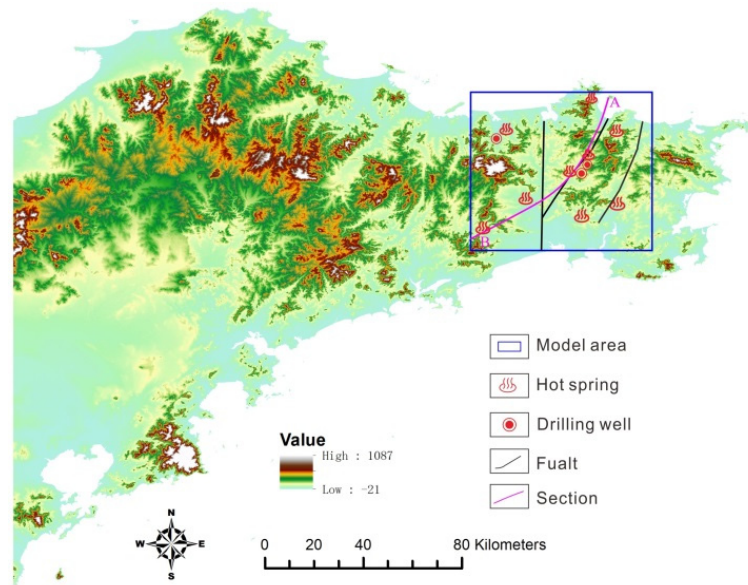


FIGURE 9: Model area of the Weihai uplift

For the surface data, the geological map in scale 1:500 000 was used. The main faults in this area are the Mishan fault, the Wenquan fault and the Xizicheng fault. Together with the hot springs and borehole wellhead locations the coordinates were inserted into Leapfrog. The subsurface information consists of the lithology in the Weihai uplift which is relatively simple with a very thin Quaternary sand layer at the surface and granite. In this area, 9 hot springs and 3 boreholes with temperature logs and lithology data were used to build the model. The boundaries of the model are listed in Table 2.

TABLE 2: Boundary of the modelling area

Items	Min.	Max.
X (east)	380861.6	448932.7
Y (north)	4096220.0	4154780.0

### 4.2 Stratigraphic model

In the Weihai uplift area, granite is widely distributed and the Quaternary sand layer is very thin, less than 50 m in the geothermal field. Therefore, the lithology in the stratigraphic model can be divided into two layers, the top sand and the granite below. Since the sand layer is very thin compared to the granite, it is not possible to show that layer in this model. The main faults are the Mishan fault, the Wenquan fault and the Xizicheng fault (Figure 10).

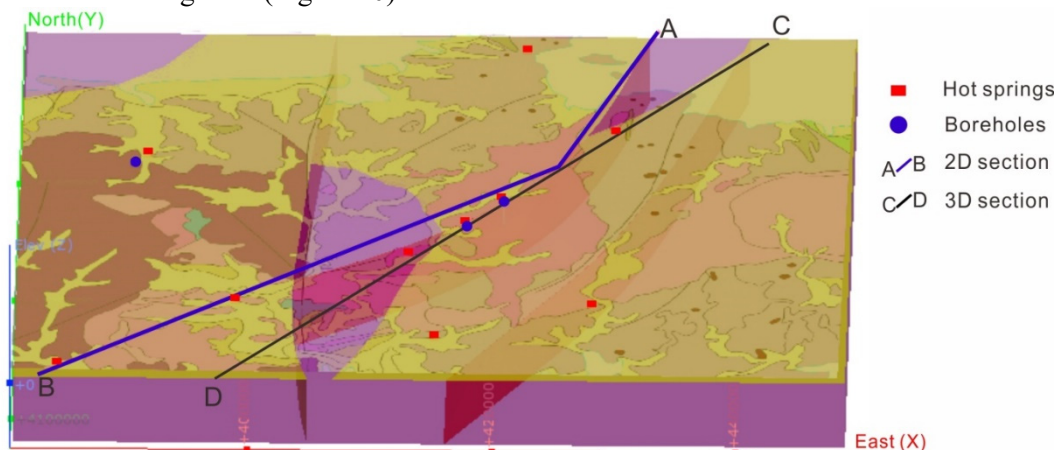


FIGURE 10: Stratigraphic model in the Weihai uplift area (see Figure 9 for location)

### 4.3 3D model of Weihai uplift

Temperature data has been used to create a 3D temperature model which has shed light on the importance of major geological structures and how they relate to heat flow in the area (Figure 11). As can be seen from Figure 11, the hot springs are mainly aligned along the Wenquan fault. The temperature along the Wenquan fault is much higher than in other locations in the model area. The temperature is highest at the Hongshuilan Tang hot spring along the Wenquan fault (Figure 12).

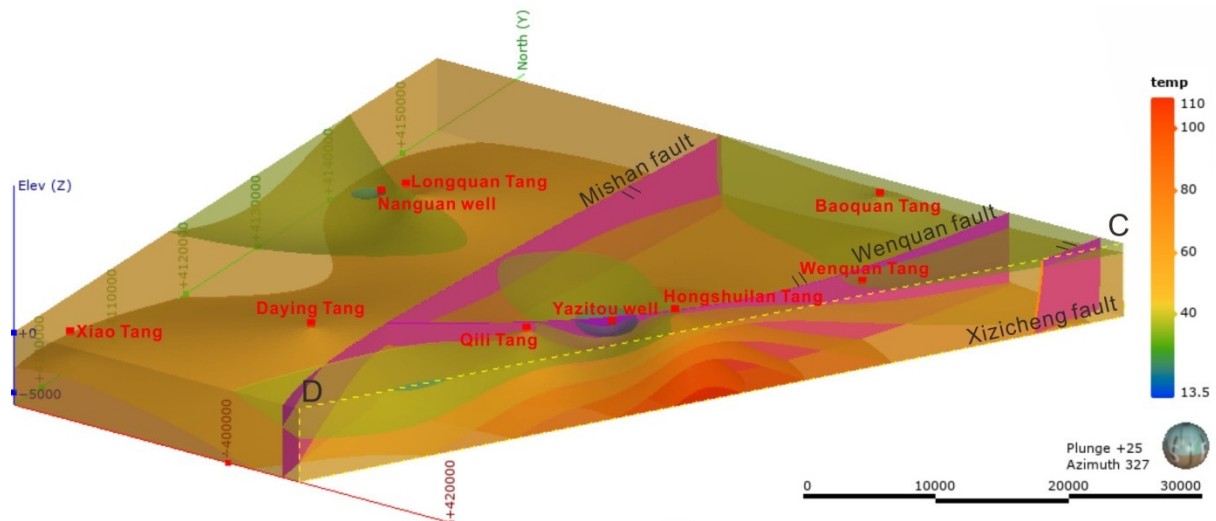


FIGURE 11: 3D temperature model of the Weihai uplift with the Mishan fault, the Wenquan fault, and hot springs (see Figure 10 for location)

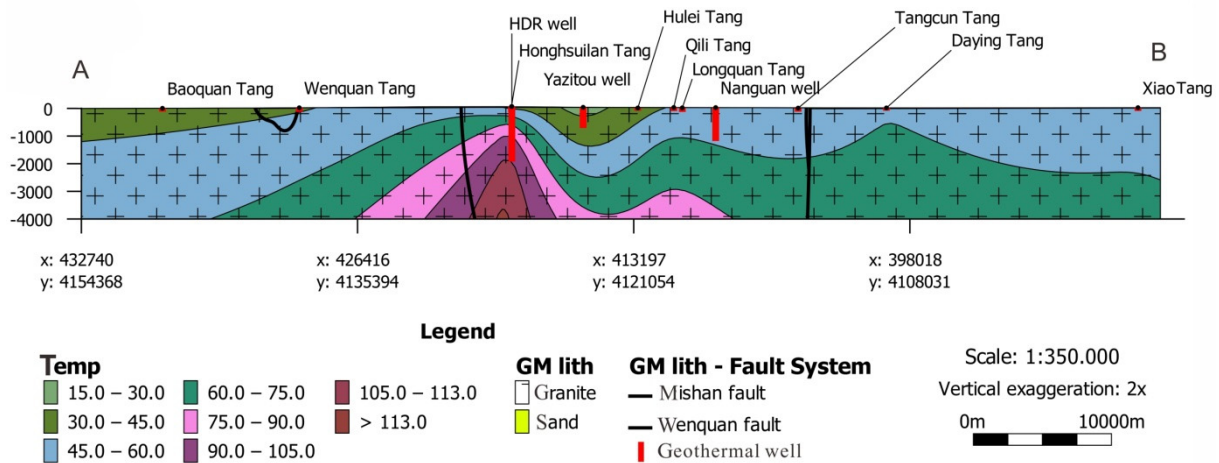


FIGURE 12: Temperature section A-B (see Figure 10 for location)

## 5. CONCEPTUAL MODEL

### 5.1 Main parameters

The factors influencing the shallow temperature field on the Jiaodong peninsula include structural distribution, thermal properties of rocks in different strata, heat storage distribution, and groundwater hydrology. Due to the strong activity of the upper mantle and the crustal movement during the Yanshanian period during the formation process of the Jiaobei uplift and the Weihai uplift, the central axis position became more fractured relative to the two wing positions affected by the compressive stress.

There are series of NE-SW and NNE-SSW faults, and the lithology is mainly composed of monzonitic granites from the Mesozoic, Archean and Proterozoic period. The research shows that the thermal conductivity increases nonlinearly with the increase of axial pressure. The higher the porosity, the higher the thermal conductivity of granite (Durutürk et al., 2002; Zhao et al., 1995; Chen et al., 2016). Therefore, on the Jiaodong peninsula where granite is widely distributed, the more fractured the uplift axis and the higher the thermal conductivity in the fault zone, the faster the heat transfer. The fracture zones also provide channels for the upwelling of deep heat flow.

The thermophysical parameters of rocks mainly refer to the physical properties such as thermal conductivity, thermal diffusivity, specific heat capacity and radioactive heat generation rate, and are important indicators for characterizing the thermophysical properties (Xu, 1992). The thermophysical properties of rocks directly affect the thermal generation, storage and transmission of heat between the various layers. They are indispensable parameters for the study of temperature distribution and heat transfer (Song et al., 2019).

The lithology of the Jiaobei uplift and the Weihai uplift is dominated by granitic intrusive rocks. The average thermal conductivity of granite is 2.6 – 3.6 W/m<sup>2</sup>K (Jiang et al., 2016). Thermal conductivity of granitic rocks in the Jiaodong uplift area is between 2.2 and 3.6 W/m<sup>2</sup>K. The thermal conductivity of acidic rock and basic rocks is approximately 2.5 W/m<sup>2</sup>K (Wang et al., 2015). The Jiaolai basin is dominated by sandstone which has a lower thermal conductivity than granite at 1.8 W/m<sup>2</sup>K. Its permeability is even lower than that of the highly fractured granite in the area (Zhou et al., 2011).

The shape of the reservoir and geothermal fluid movement are also main factors affecting the distribution of local geothermal fields. The reservoir shape determines the flow space of the fluid inside the earth. While the geothermal fluid is carrying heat, it also affects the distribution of temperature around the reservoir. This is the main reason of local thermal anomalies on the surface of the Jiaodong peninsula.

## 5.2 Heat flow distribution

The intrusive rocks, deep faults and dike rock in the area are very developed. The current hot springs are mainly located on the axis and two wings of the Jiaobei and Weihai uplift, while there are no hot springs in the Jiaolai basin. It can be seen in Figure 4 that the value of the heat flow according to silica temperatures in the uplift area is significantly higher than in the depression. All the boreholes in the Jiaodong peninsula have normal temperature gradients (Figure 7), indicating no heat source. The geothermal resources in the Jiaodong peninsula are low- to medium-temperature convective geothermal resources controlled by faults. The difference in the heat flow is caused by its difference in structural units.

## 5.3 Conceptual model

Figure 13 illustrates how, in the process of upwelling, the heat flow from the interior of the earth first reaches the Moho surface before entering the crust. When the deep heat flow reaches this interface, it seems to be rather uniform. However, due to the lithology in the uplift area being granite, but sandstone in the basin, the difference in the thermal conductivity and permeability of the different rocks causes the bottom of Jiaolai basin to become a heat and water insulation surface (Figure 13). When the heat flow reaches this interface, the heat flow deflects to both sides (the uplift areas), where higher thermal conductivity and better permeability is present. The rising heat flow accumulates in the uplift areas causing higher temperatures.

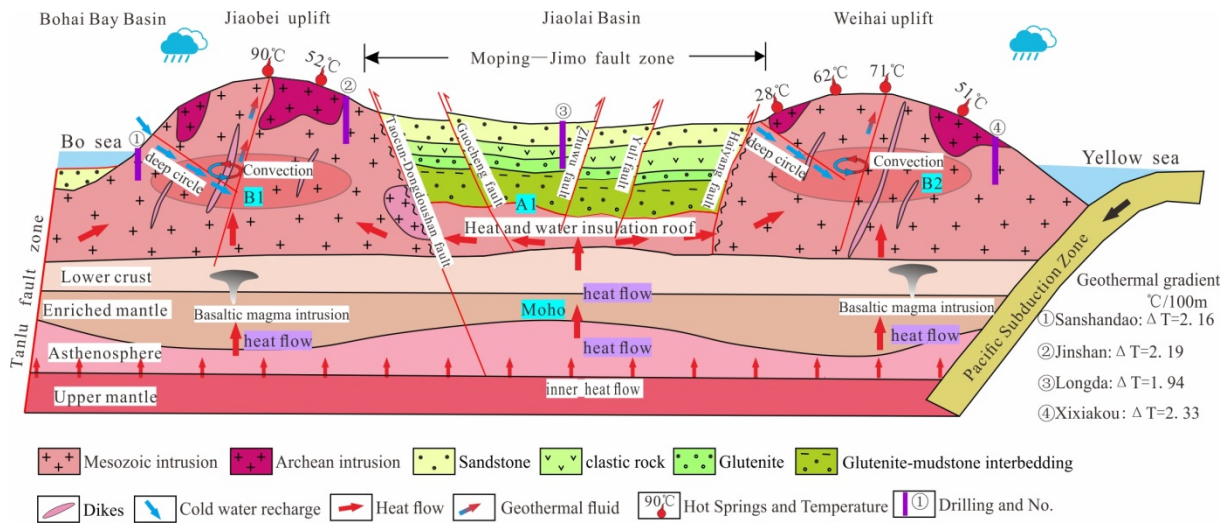
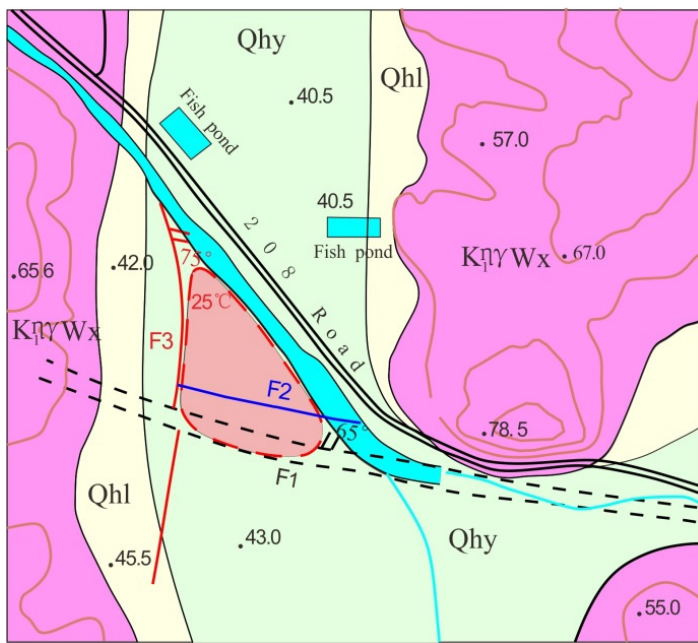


FIGURE 13: Conceptual model of heat flow in uplifts and depression on the Jiaodong peninsula

6. LUMPED PARAMETER MODELLING FOR YUJIA TANG AREA

The software Lumpfit was developed by Axelsson and Arason (1992). Lumped parameter modelling is a simple method for simulating pressure changes in geothermal reservoirs during production which can be used to estimate production capacity. Lumpfit can simulate water level or pressure change with lumped parameter models and predict water level or pressure histories very accurately provided data quality is sufficient.

Lumped parameter modelling is used here to assess the sustainable production capacity of the Jiaodong geothermal reservoir through predictions of water level response to changes in production load.



1. Fine sand of Yihe Formation    2. Coarse sand of Linyi Formation  
 3. Yanshanian monzonitic granite    4. Geothermal field range  
 5. 25-degree isotherm    6. Fault of different properties

FIGURE 14: Geological map of the Yujia Tang area including faults (F1, F2 and F3) and location of the geothermal field

6.1 The geothermal area – overview

The Yujia Tang geothermal field is located in Yujiatang village, Laishan district, Yantai city, Shandong province. It is classified as a low- to middle-temperature convective geothermal field controlled by faults. The geothermal system includes a complete path of recharge, runoff and outflow and is an open geothermal system.

Figure 14 shows that the lithology of the geothermal field is relatively simple, mainly composed of monzogranite from the late Yanshanian of the Mesozoic. The surface of the geothermal field is covered with fine sand of the Yihe formation and coarse sand of the Linyi formation. There are three main faults controlling the



geothermal field. F1 is the main fault zone in this area. Its strike is NW-SE and it slopes towards northeast with an inclination of  $\sim 60-70^\circ$ . Its width is about 20 m and the fault-zone includes breccia and fault mud. The F1 fault is believed to act as a flow barrier. The F2 fault also strikes NW-SE, sloping to northeast, with a width of about 10 m. It is a secondary fault to the F1 fault and considered to be a water-conducting (permeable) fault. F3 is a NNE-SSW oriented compression-torsion fault. The high-permeability fracture zone formed by the intersection of the F2 and F3 faults provides a channel for the up flow of the geothermal fluids, forming the geothermal fluid channel of the Yujia Tang geothermal field. In this study, we define the boundary of the geothermal field by the  $25^\circ\text{C}$  temperature isotherm. The geothermal wells in this geothermal field are mainly distributed in the north of F2 and west of F1 and there is no obvious geothermal anomaly at the foot walls of faults F1 and F3.

At present, there are 6 production wells in the Yujia Tang geothermal area. The depth of the wells is 100-200 m and the main utilization is bathing, as well as fish-farming and heating. The current average production is about  $1000 \text{ m}^3/\text{d}$  (11.6 l/s), the wellhead water temperature is  $46^\circ\text{C}$ , and the historical maximum production is  $4000 \text{ m}^3/\text{d}$  (46 l/s).

## 6.2 Long-term observational data

At present, with the increase of geothermal fluid extraction, the water level and water temperature of the Yujia Tang geothermal field have declined to some extent. According to observation data of Yujia Tang geothermal field in 1965, the geothermal field was self-flowing at that time with a flow rate of  $294 \text{ m}^3/\text{d}$  (3.4 l/s).

Since 2006, continuous monitoring data is available for the Yujia Tang geothermal field (Figure 15). It shows that during the summer with small production the well can be self-flowing, but in winter with high production the well water level drops considerably.

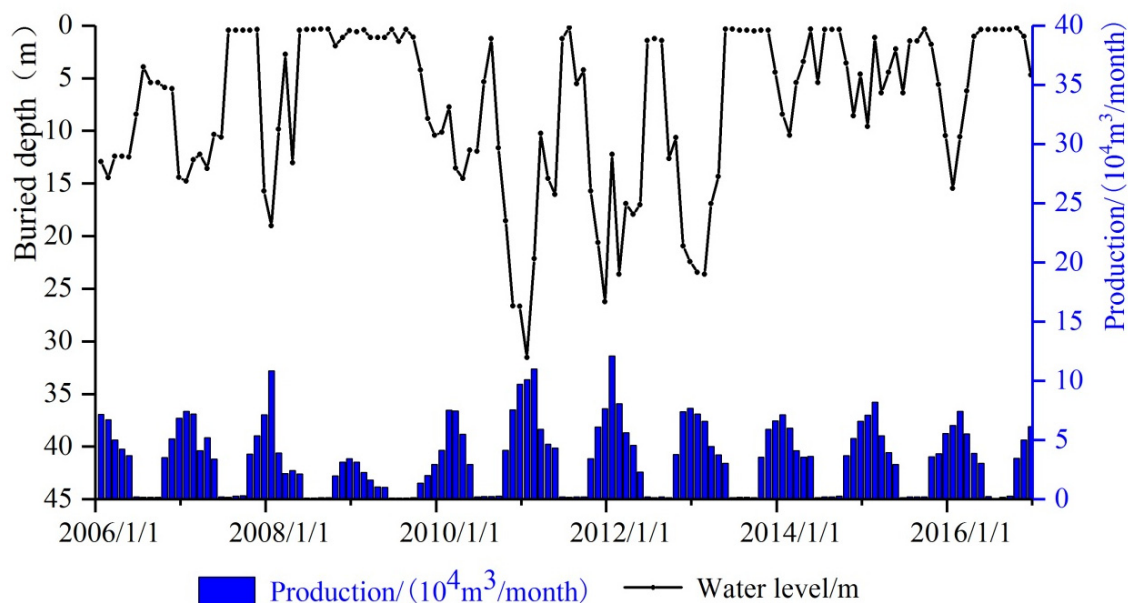


FIGURE 15: Water level and exploitation of the Yujia Tang geothermal area from 2006 to 2016

## 6.3 Modelling and forecast

Because the Yujia Tang geothermal system is an open geothermal system, it shows the complete process of recharge, runoff, and out flow. So, in the Lumpfit model we use the open one-tank model to simulate

water level change and predict the production, instead of the closed model which would be more pessimistic. The results of the lumped parameter modelling are presented in Figure 16.

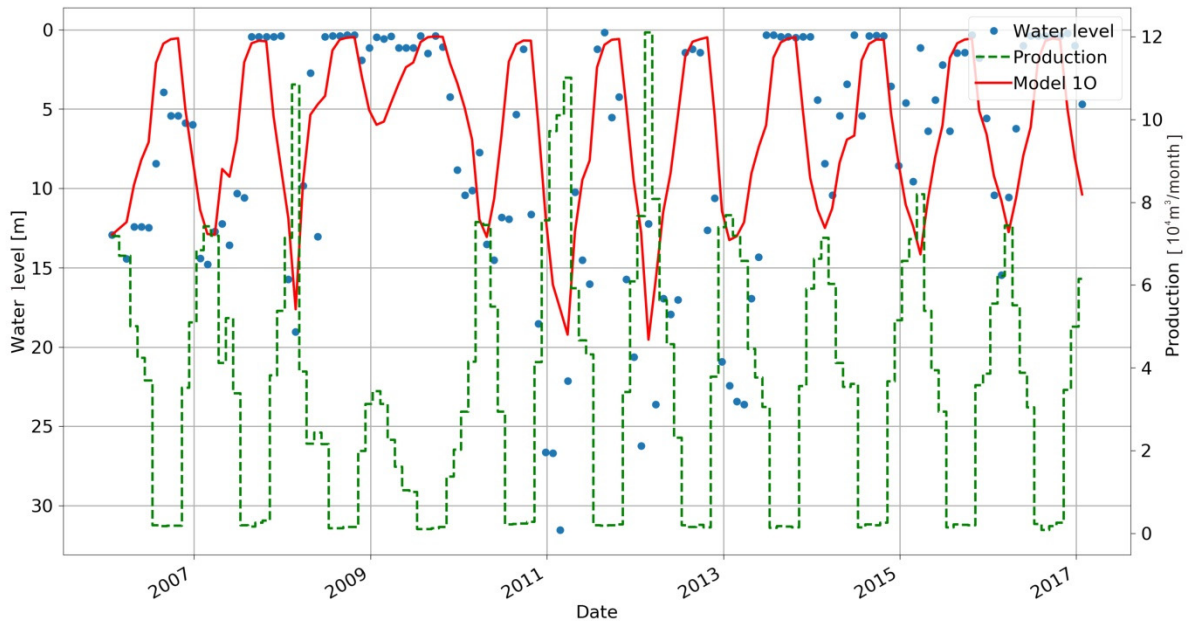


FIGURE 16: Observed water level and production data and simulated results using one-tank open lumped model

Table 3 presents production data for the Yujia Tang geothermal field. In order to create accurate forecasts for the water level behaviour, for each month the average production from the last ten years is used. This considers seasonal behaviour.

TABLE 3: Production data for the Yujia Tang field; original data shows average values for the last ten years while the last 3 columns are used for predictions ( $10^4 \text{ m}^3/\text{mon.}$ )

Months	Original data	5 times	10 times	15 times
January	7.51	37.5	75.1	112.6
February	6.65	33.3	66.5	99.8
March	4.67	23.3	46.7	70.0
April	3.89	19.4	38.9	58.3
May	2.95	14.7	29.5	44.2
June	0.17	0.85	1.70	2.55
July	0.16	0.80	1.60	2.40
August	0.19	0.95	1.90	2.85
September	0.21	1.05	2.10	3.15
October	3.30	16.5	33.0	49.5
November	5.14	25.7	51.4	77.1
December	6.39	31.9	63.9	95.9

In order to show the water level change with the production increase, the production is increased to 5, 10, and 15 times the original rate. Figures 17-20 show measured water levels and production together with the model simulations as well as the model predictions for the next 10 years.

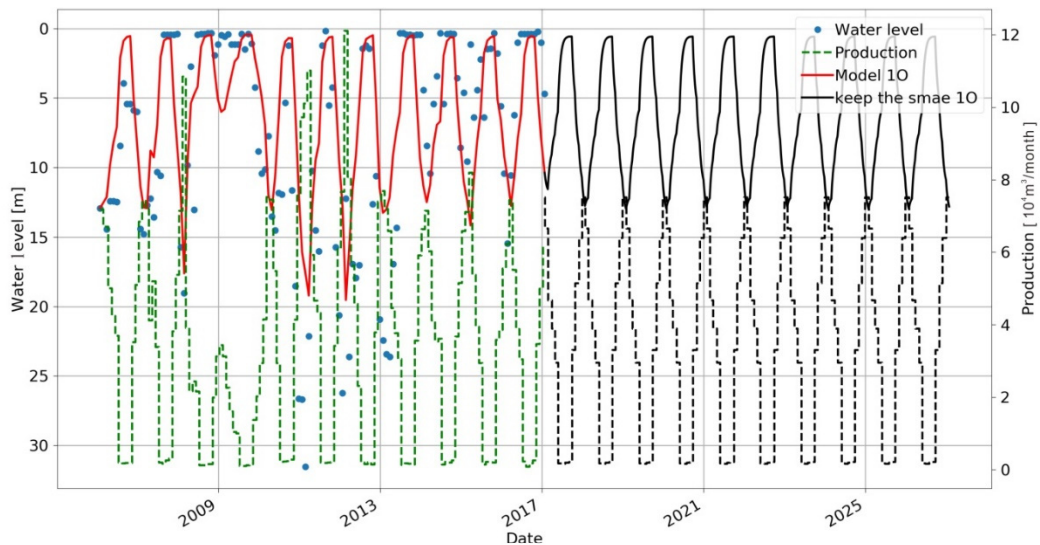


FIGURE 17: Prediction for 10 years with current production using a one-tank open model

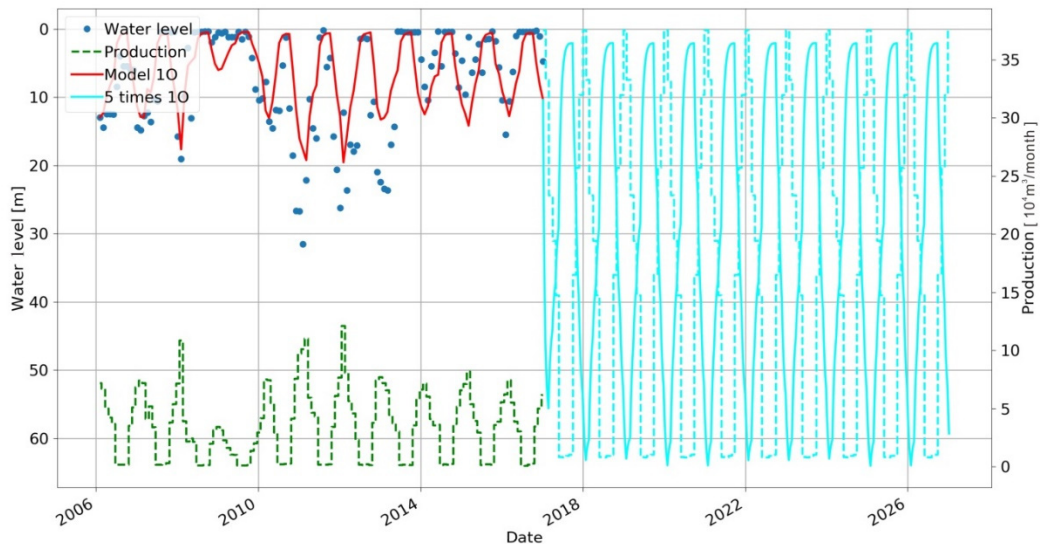


FIGURE 18: Prediction for 10 years with 5 times current production using a one-tank open model

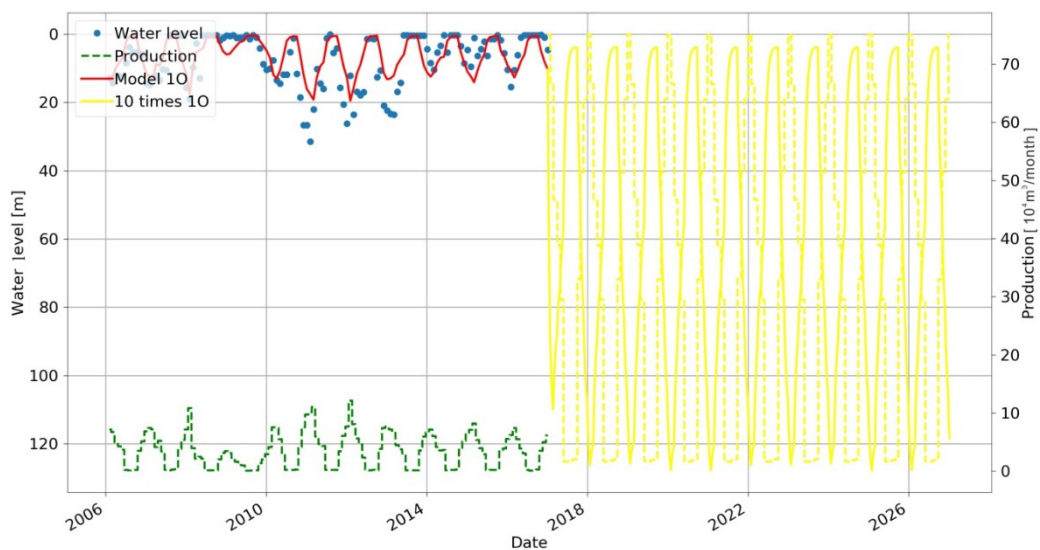


FIGURE 19: Prediction for 10 years with 10 times current production using a one-tank open model

In Figure 17 we can see that if the current production status is kept, the water level will drop by 14 m. When the production increases to 5 times the present production, the water level will drop 62 m (Figure 18), and when it increases to 10 times the present production, the water level will drop 125 m (Figure 19). Finally, when it increases to 15 times the present production, the water level will drop 180 m (Figure 20). If the limit is set at a maximum water level drop of 180 m, the production cannot exceed 15 times the current production.

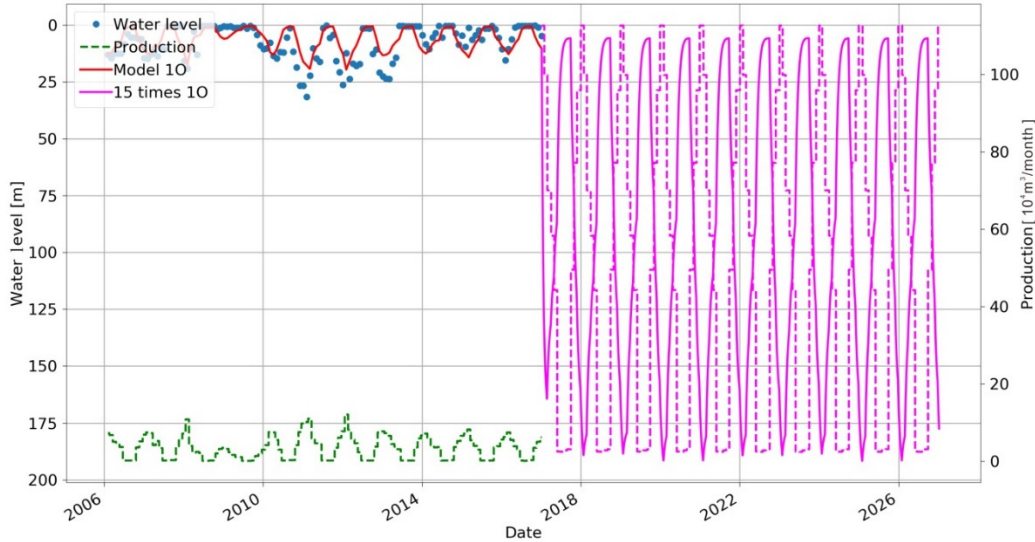


FIGURE 20: Prediction for 10 years with 15 times current production using a one-tank open model

## 7. GEOTHERMAL RESOURCE ASSESSMENT

The volumetric method using simple stored heat models, adapted from mineral exploration and oil industry, can estimate the total energy content in a geothermal system and how much of that can be extracted over a given time. It can give useful estimates even when few wells have been drilled. The volumetric method is usually used for a first assessment of the geothermal resource (Tulinus, 2019).

The volumetric method involves calculation of the total heat energy stored in a volume of formation compared to a reference temperature. Most of the time this method is used for electrical generation purposes, but it can also be used to calculate the thermal energy in the reservoir. Total thermal energy is the sum of energy stored in the rock matrix and thermal energy of fluid in rock pores, given by:

$$E_{res} = E_{rock} + E_{fluid} \quad (2)$$

$$E_{rock} = V(1 - \phi)\rho_{rock} \times K_{rock} \times (T_{res} - T_{ref}) \quad (3)$$

$$E_{fluid} = V\phi\rho_{fluid} \times K_{fluid} \times (T_{res} - T_{ref}) \quad (4)$$

where  $\rho$  is density ( $\text{kg/m}^3$ );  
 $K$  is heat capacity ( $\text{J/kg}^\circ\text{C}$ );  
 $V$  is reservoir volume ( $\text{m}^3$ );  
 $E$  is energy (J);  
 $T_{res}$  is reservoir temperature ( $^\circ\text{C}$ );  
 $T_{ref}$  is rejection or cut-off temperature ( $^\circ\text{C}$ ), and  
 $\phi$  is porosity (fraction).

Total recoverable thermal energy  $E_{recoverable}$  is given by:

$$E_{recoverable} = A \times R \times E_{res} \quad (5)$$



where  $A$  is accessibility; and  
 $R$  is recovery factor.

## 7.1 Input parameters

As we know, on the Jiaodong peninsula, the geothermal resources are of low temperature type. Most of the time they are just used for bathing and to a smaller extent for heating and fish farming but not for power generation. In this part, we take the Wenquan Tang field in Weihai city in the Weihai uplift area and the Dong Tang field in Zhaoyuan city in the Jiaobei uplift, as examples to calculate the total energy in the respective reservoirs.

Table 4 shows the parameters used for the two geothermal fields on Jiaodong peninsula. The data is mainly adopted from the report of the Shandong Provincial Bureau of Geology & Mineral Resources (Zhang, 2008). In it, the area, thickness, temperature and density of water are derived from measured data. Because the lithology of the reservoirs on the Jiaodong peninsula involves granites and monzonitic granites, the porosity is assumed to be 10%, the specific heat of rock is assumed to be 795 J/kg°C, and the density of rock 2700 kg/m<sup>3</sup>. The specific heat of water is 4200 J/kg°C.

TABLE 4: Data and various parameters used in the volumetric assessments for the Wenquan Tang and Dong Tang geothermal fields

Name	Area (km <sup>2</sup> )	Thickness (m)	Porosity	Temp (°C)	Specific heat of rock (J/kg°C)	Density of rock (g/cm <sup>3</sup> )	Specific heat of water (J/kg°C)	Density of water (g/cm <sup>3</sup> )
Wenquan Tang	0.43	200	0.25	126	795	2.70	4200	987
Dong Tang	0.36	220	0.25	128	795	2.70	4200	967

On the Jiaodong peninsula the geothermal water is used for bathing, so there is no reinjection and the average yearly ambient temperature of 14°C is used as the cut-off temperature. The efficiency of thermal energy extraction is 100%. Combined with the development degree of reservoir fissures in the geothermal systems, it was determined that the recovery factor is 0.15. The load factor is assumed to be 0.95. Input parameters used for volumetric calculations of the Wenquan Tang and Dong Tang geothermal areas are listed in Tables 5 and 6. The Monte Carlo method is used to incorporate uncertainty on the main parameters, which is considerable. Hence, many of the parameters are presented as minimum, maximum and best values.

TABLE 5: Input parameters used for volumetric resource assessment for the Wenquan Tang geothermal system

Input variables	Unit	Min	Best Value	Max
Area	km <sup>2</sup>	0.30	0.43	0.50
Thickness	m	150	200	300
Reservoir temperature	°C	120	126	130
Porosity	%	5	10	15
Specific heat capacity of rock	J/(kg°C)	NA	795	NA
Density of rock	kg/m <sup>3</sup>	NA	2,700	NA
Specific heat capacity of water	J/(kg°C)	NA	4,200	NA
Density of water	kg/m <sup>3</sup>	NA	987	NA
Recovery factor	%	5	15	20
Cut-off temperature	°C	NA	14	NA
Efficiency	%	NA	100	NA
Load factor	%	NA	95	NA

TABLE 6: Input parameters used for volumetric resource assessment for the Dong Tang geothermal system

Input variables	Unit	Min	Best Value	Max
Area	km <sup>2</sup>	0.30	0.36	0.50
Thickness	m	150	220	300
Reservoir temperature	°C	120	127	130
Porosity	%	5	10	15
Specific heat capacity of rock	J/(kg°C)	NA	795	NA
Density of rock	kg/m <sup>3</sup>	NA	2,700	NA
Specific heat capacity of water	J/(kg°C)	NA	4,200	NA
Density of water	kg/m <sup>3</sup>	NA	987	NA
Recovery factor	%	5	15	20
Cut-off temperature	°C	NA	14	NA
Efficiency	%	NA	100	NA
Load factor	%	NA	95	NA

## 7.2 Volumetric resource assessment results

For the Wenquan Tang geothermal system, the 90% percentile of the Monte Carlo calculation results (P90) is 2.1 MW<sub>th</sub> and for 50% it is 3.2 MW<sub>th</sub> (P50). The cumulative histogram output for the calculation is shown in Figure 21. For the Dong Tang geothermal system, the 90% percentile (P90) is 2.1 MW<sub>th</sub> and for 50% it is 3.4 MW<sub>th</sub>. The cumulative histogram output for the calculation is shown in Figure 22.

From the results for the two fields it can be seen that the energy production capacity for comparable small fracture-controlled low- to medium-temperature geothermal systems can be expected to be around 2-3 MW<sub>th</sub>.

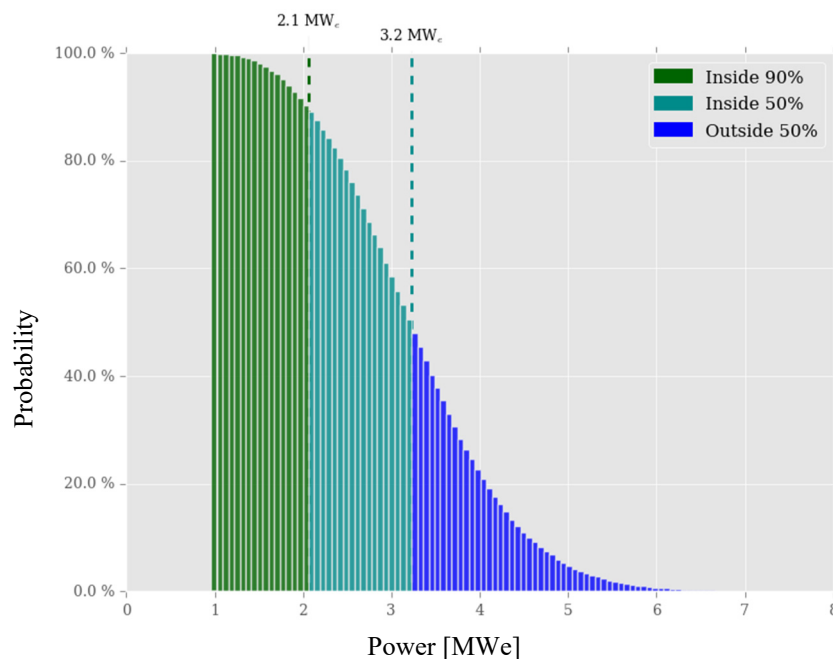


FIGURE 21: Cumulative probability of the thermal energy capacity of the Wenquan Tang geothermal field according to a Monte Carlo volumetric assessment

## 8. CONCLUSIONS

This report presents an analysis of the heat flow distribution, logging data from wells and the thermophysical parameters of rocks on the Jiaodong peninsula. A 3D model of temperature and lithology is consequently presented and a general conceptual model established. Lumped parameter modelling of observed water-level changes for a small-scale example, as well as volumetric geothermal resource assessment for two other examples are presented. The main conclusions of the project are:

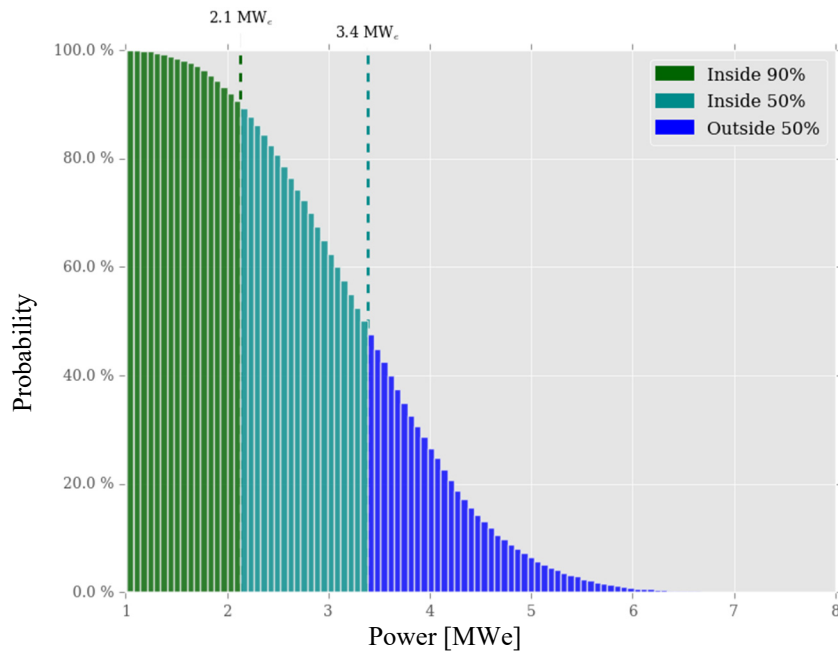


FIGURE 22: Cumulative probability of the thermal energy capacity of the Dong Tang

1. The lithology in uplift areas of the peninsula mainly involves granite while in the basin in-between it is mainly composed of sandstone. The heat-flow in the uplift areas is much higher than in the basin. This is partly due to the difference of thermophysical parameters of different rocks, causing heat flow to change direction and redistribute along the bottom of the basin to both sides – to the uplifts. This causes the uplift areas to have higher heat flow.
2. The geothermal fluids on the Jiaodong peninsula are mainly heated by terrestrial heat flow and heat-transporting faults. There are no high-temperature heat sources like magmatic intrusions in this area.
3. The long-term monitoring data of the Yujia Tang geothermal field demonstrates that in summer, when production is low, the production well can recover to self-flow, even if the production is increased to 15 times the current production, based on lumped parameter modelling. If the limit is set so that the water level may not drop more than 180 m in winter, the production cannot be increased more than 15 times the current production.
4. The geothermal systems on the Jiaodong peninsula are low- to medium-temperature geothermal resources and are mainly used for bathing and heating rather than electrical power generation. Using the volumetric method with Monte Carlo calculations, it is estimated that the thermal energy production capacity of the Wenquan Tang and Dong Tang geothermal systems is around 2–3 MW<sub>th</sub> (P90 estimate).

## 9. RECOMMENDATIONS

1. On the Jiaodong peninsula, most of the geothermal wells belong to private owners or different companies, and therefore it is difficult to monitor the geothermal system or do research. The geothermal water level and temperature have declined, so it would be beneficial if the government managed the geothermal field to enable sustainable development.
2. The geothermal fields on the Jiaodong peninsula are very small and geophysical exploration has not been carried out in the geothermal fields. Therefore, there is a lack of the geophysical data

and it is difficult to do research in this area. In the future, more geophysical exploration should be done covering all the area and not only the geothermal fields.

3. The depth of the boreholes in the geothermal field is mostly less than 300 m, which is very shallow. Deeper drilling could lead to higher energy output.

## ACKNOWLEDGEMENTS

I would like to express my great gratitude to Director Lúdvík S. Georgsson for offering me the precious opportunity to attend this six-month training. Thanks all the staff of UNU-GTP for your help here, Ms. Málfríður Ómarsdóttir, Mr. Ingimar G. Haraldsson, Mr. Markús A.G. Wilde, Dr. Vigdís Hardardóttir and Ms. Thórhildur Ísberg.

I would like to thank Dr. Svanbjörg Helga Haraldsdóttir, Dr. Gudni Axelsson, and Ms. Helga Tulinius from ÍSOR for their supervision and guidance for my personal project. They provided me with patient guidance and advice even though my English is not very good.

Thanks to my supervisor at home, Dr. Kang Fengxin, who gave me chance to participate in the meeting with Lúdvík and opened up the opportunity to go to Iceland. Thanks to my employer, Shandong No. 3 Exploration Institute of Geology and Mineral Resources, to allow me to study here.

Thanks to all the UNU fellows, they helped me a lot to speak English and gave me encouragement. Special thanks to Vivi and Erick who give me a lot of help in my project and daily life. Also thanks a lot to my roommates Erick, Muba and John, they are funny guys and are like a family to me.

Finally, thanks a lot to my wife and mother for taking care of my 4-month old daughter and the support they provided me with during this training.

## REFERENCES

- Axelsson, G. and Arason, P., 1992: *LUMPFIT: Automated simulation of pressure changes in hydrological reservoirs, version 3.1, user's guide*. Orkustofnun, Reykjavík, 32 pp.
- Alcaraz, S., Lane, R., Spragg, K., Milicich, S., Sepulveda, F. and Bignall, G., 2011: 3D geological modelling using new Leapfrog geothermal software. *Proceedings of the 36<sup>th</sup> Workshop on Geothermal Reservoir Engineering, Stanford University, Stanford, CA*, 31 pp.
- Chen B., Chen C., Kaban, M.K., Du J., Liang Q., and Thomas, M., 2013: Variations of the effective elastic thickness over China and surroundings and their relation to the lithosphere dynamics. *Earth and Planetary Science Letters*, 363, 61-72.
- Chen M., Huang G. and Xiong L., 1988: *North China geothermal (in Chinese)*. Science Press, Beijing, 218 pp.
- Chen M., Wang J., Wang J., Deng X., Yang S., Xiong L. and Zhang J., 1990: The characteristics of geothermal fields and their formation mechanism in the North China down-faulted basin (in Chinese). *Acta Geologica Sinica*, 1, 80-91.
- Chen Y., Pirajno, F., Lai Y. and Li C., 2004: Metallogenic time and tectonic setting of the Jiaodong gold province, Eastern China (in Chinese). *Acta Petrologica Sinica*, 20-4, 907-922.
- Chen Z., Wu X., Chen F., Wang H., and Sun D., 2016: Research of thermal conductive characteristics of granite under uniaxial compression (in Chinese). *Coal Engineering*, 48-9, 113-116.



- Deng J., Zhai Y., Yang L., Xiao R., and Sun Z., 1999: Tectonic evolution and dynamics of metallogenic systems – An example from the gold ore deposits concentrated area in Jiaodong, Shandong, China (in Chinese). *Earth Science Frontiers*, 6-2, 315-323.
- Durutürk, Y.S., Demirci, A., and Keçeciler, A., 2002: Variation of thermal conductivity of rocks with pressure. *CIM Bull*, 95, 67-71.
- Fournier R. O. (1977): Chemical geothermometers and mixing models for geothermal systems. *Geothermics*, 5, 41-50.
- Hu S., and Wang J., 1994: Heat flow characteristics of orogenic belts in southeastern China (in Chinese). *Geological Review*, 40-5, 387-394.
- Jiang G., Tang X., Rao S., Gao P., Zhang L., Zhao P., and Hu S., 2016: High-quality heat flow determination from the crystalline basement of the south-east margin of North China Craton (in Chinese). *J. Asian Earth Sciences*, 118, 1-10.
- Jin B., Zhang Y., and Luan G., 1999: Characteristics of geothermal resources in Jiaodong Peninsula (in Chinese). *Ludong University Journal (Natural Science Edition)*, 15-4, 297-301.
- Li X., Liu B., Sun X. and Wang Y. 1997: Relationship between the silica heat flow and regional geological conditions in Shandong Peninsula (in Chinese). *J. of Ocean University of Qingdao*, 27-1, 75-83.
- Li Z., Gao J., Li W., and Wu J., 2016: The characteristics of geothermal field and controlling factors in Qaidam Basin, Northwest China (in Chinese). *Earth Science Frontiers*, 23-5, 23-32.
- Lin S., Zhu G., Yan L., Jiang Q., and Zhao T., 2013: Discussion on uplifting mechanism of the Linglong batholith in the Jiaodong Region (in Chinese). *Geological Review*, 59-5, 832-844.
- Liu C., Deng J., Li S., Xiao Q., Jin T., Sun H., Di Y., Liu Y., and Zhao G., 2018: Discussions on crust-mantle structure during the formation of Yanshanian of large and super-large scale deposits in the Jiaodong gold ore district: Constraints from ore-forming igneous assemblage (in Chinese). *Earth Science Frontiers*, 25-6, 296-307.
- Liu S., Li X., Hao C., and Li X., 2017: Heat flow, deep formation temperature and thermal structure of the Tarim Basin, North China (in Chinese). *Earth Science Frontiers*, 24-3, 41-55.
- Long Q. 2017: *A geochemical study of Mesozoic intermediate to mafic dykes in the Jiaodong peninsula (in Chinese)*. University of Science and Technology of China, Hefei city, 185 pp.
- Lv G., Guo T., Shu B., Shen Y., Liu D., and Zhou G., 2007: Study on the multilevel controlling rule for tectonic system in Jiaodong gold centralized area (in Chinese). *Geotectonica et Metallogenia*, 31-2, 193-204.
- Lv C., Wu G., Maerz, N.H., and Boyko, K.J., 2015: A study of distribution and charge of regional tectonic fluid in goldfields of Jiaodong Peninsula (in Chinese). *Earth Science Frontiers*, 22-4, 113-121.
- Mao J., Li H., Wang Y., Zhang C., and Wang Y., 2005: The relationship between mantle-derived fluid and gold ore-formation in the Eastern Shandong Peninsula: Evidences from D-O-C-S isotopes (in Chinese). *Acta Geologica Sinica*, 79-6, 839-857.
- Pan S., Wang F., Zheng Y., Duan Y., Liu L., Deng X., Song X., Sun Y., and Ma C., 2015: Crustal velocity structure beneath Jiaodong Peninsula and its tectonic implications (in Chinese). *Chinese J. Geophysics*, 58-9, 3251-3263.
- Qiu N., Xu W., Zuo Y., Chang J., and Liu C., 2017: Evolution of Meso-Cenozoic and thermal-rheological structure of the lithosphere in the Bohai Bay Basin, eastern North China Craton (in Chinese). *Earth Science Frontiers*, 24-3, 13-26.

- Shi X., Yu C., Chen M., Yang X., and Zhao J., 2017: Analysis of variation features and influential factors of heat flow in the northern margin of the South China sea (in Chinese). *Earth Science Frontiers*, 24-3, 56-64.
- Song X., Jiang M., Peng Q., and Xiong P., 2019: Thermal property parameters and influencing factor analysis of main rock strata in Guizhou province (in Chinese). *Acta Geologica Sinica*, 93-8, 2092-2103.
- Tan J., Wei J., Yang C., Feng B., Tan W., and Guo D., 2006: Geochemistry and tectonic setting of dikes in the Guocheng area, Jiaodong Peninsula (in Chinese). *Acta Geologica Sinica*, 80-8, 1177-1188.
- Tulinius, H., 2019: *Volumetric resource assessment*. UNU-GTP, Iceland, unpublished lecture material.
- Wang A., Sun Z., Liu J., Hu B., Wan J., and Yang L., 2015: Radiogenic heat production of rocks from Zhangzhou, Southeast China and its implications for thermal regime of lithosphere (in Chinese). *Science & Technology Review*, 33-24, 41-45.
- Wulaningsih, T., Fujii, Y., Tsutsumi, S., Inagaki, H., Umeo, Y., and O'Brien, J., 2017: A 3D model of the Yamagawa geothermal system: Insights into reservoir structure and future field management. *Proceedings of 39<sup>th</sup> New Zealand Geothermal Workshop, Auckland*, 7 pp.
- Xie X., and Yu H., 1988: The characteristics of the regional geothermal field in Sichuan Basin (in Chinese). *Journal of Chengdu College of Geology*, 4, 110-117.
- Xiong L. and Zhang J. 1984: Mathematical simulation of refraction and redistribution of heat flow (in Chinese). *Chinese Journal of Geology*, 4, 445-454.
- Xu Z., 1992: A discussion of factors influencing thermophysical characteristics of rocks and their mechanisms (in Chinese). *Petroleum Exploration and Development*, 19-6, 85-89.
- Zhang H., 2008: *Geothermal resource survey and evaluation in Jiaodong area, Shandong Province*. Qingdao Geological Engineering Survey Institute, Qingdao City, 179 pp.
- Zhang J., Sun H., and Xiong L., 1982: Mathematical simulating of regional geothermal field and case analysis (in Chinese). *Chinese Journal of Geology*, 3, 315-321.
- Zhang T., 2011: Study on hydrochemistry and isotopic characteristics of geothermal water in Jiaodong peninsula (in Chinese). *Land and Resources in Shandong Province*, 27-12, 11-16.
- Zhang T., and Zhang Y. 2007: Geochronological sequence of Mesozoic intrusive magmatism in Jiaodong Peninsula and its tectonic constraints (in Chinese). *J. China Universities*, 13-2, 323-336,
- Zhang Y., Li J., Liu Z., Ren F., and Yuan J., 2006: Detachment systems in the deep part of Jiaolai basin and their regional tectonic significance (in Chinese). *Oil & Gas Geology*, 27-4, 504-511.
- Zhang Y., Li J., Zhang T., and Yuan J., 2007: Late Mesozoic kinematic history of the Muping-Jimo fault zone in Jiaodong Peninsula, Shandong Province, East China (in Chinese). *Geological Review*, 53-3, 289-300.
- Zhao Y., Yang S., Zhang W., Liang X., and Ma L., 1995: An experimental study of rock thermal conductivity under different temperature and pressure (in Chinese). *Progress in Geophysics*, 10-1, 104-113.
- Zhou Y., Ji Y., Zhang S., and Wan L., 2011: Characteristics and controlling factors on physical properties of low-permeability sandstone of the Laiyang formation in the Laiyang Sag, Jiaolai basin (in Chinese). *Acta Petrolei Sinica*, 32-4, 611-620.